Title

Microtubule-Targeting Agents Eribulin and Paclitaxel Differentially Affect Neuronal Cell Bodies in Chemotherapy-Induced Peripheral Neuropathy.

Journal

Neurotoxicity research, 32(1)

ISSN

1029-8428

Authors

Benbow, Sarah J
Wozniak, Krystyna M
Kulesh, Bridget
et al.

Publication Date

2017-07-01

DOI

10.1007/s12640-017-9729-6

Peer reviewed

HHS Public Access

Author manuscript

Neurotox Res. Author manuscript; available in PMC 2018 July 01.

Published in final edited form as:

Neurotox Res. 2017 July ; 32(1): 151–162. doi:10.1007/s12640-017-9729-6.

Microtubule Targeting Agents Eribulin and Paclitaxel Differentially Affect Neuronal Cell Bodies in Chemotherapy Induced Peripheral Neuropathy

Sarah J. Benbow[1,2], **Krystyna M. Wozniak**[3], **Bridget Kulesh**[1,2], **April Savage**[1,2], **Barbara S. Slusher**[3,4], **Bruce A. Littlefield**[5], **Mary Ann Jordan**[1,2], **Leslie Wilson**[1,2], and **Stuart C. Feinstein**[1,2]

[1]Neuroscience Research Institute, University of California, Santa Barbara, CA

[2]Department of Molecular, Cellular and Developmental Biology, University of California, Santa Barbara, CA

[3]Johns Hopkins Drug Discovery Program, Johns Hopkins School of Medicine, Baltimore, MD

[4]Departments of Neurology, Psychiatry, Neuroscience, Medicine and Oncology, Johns Hopkins School of Medicine, Baltimore, MD

[5]Eisai Inc., Andover, MA

Abstract

Chemotherapy induced peripheral neuropathy (CIPN) is a common side effect of anti-cancer treatment with microtubule targeted agents (MTAs). The frequency of severe CIPN, which can be dose limiting and even life threatening, varies widely among different MTAs. For example, paclitaxel induces a higher frequency of severe CIPN than does eribulin. Different MTAs also possess distinct mechanisms of microtubule-targeted action. Recently, we demonstrated that paclitaxel and eribulin differentially affect sciatic nerve axons, with paclitaxel inducing more pronounced neurodegenerative effects and eribulin inducing greater microtubule stabilizing biochemical effects. Here, we complement and extend these axonal studies by assessing the effects of paclitaxel and eribulin in the cell bodies of sciatic nerve axons, housed in the dorsal root ganglia (DRG). Importantly, the microtubule network in cell bodies is known to be significantly more dynamic than in axons. Paclitaxel induced ATF3 expression, a marker of neuronal stress/injury. Paclitaxel also increased expression levels of acetylated tubulin and EB1, markers of microtubule stability and growth, respectively. These effects are hypothesized to be detrimental to the dynamic microtubule network within the cell bodies. In contrast, eribulin had no significant effect on any of these parameters in the cell bodies. Taken together, DRG cell bodies and their axons, two distinct neuronal cell compartments, contain functionally distinct microtubule networks that exhibit unique biochemical responses to different MTA treatments. We hypothesize that these distinct mechanistic actions may underlie the variability seen in the initiation, progression, persistence and recovery from CIPN.

Contributing Author: Stuart C. Feinstein, Neuroscience Research Institute, University of California, Santa Barbara, CA 93106, Phone: 805-893-2659, FAX: 805-893-2005, feinstei@lifesci.ucsb.edu.

Keywords

chemotherapy-induced peripheral neuropathy; paclitaxel; eribulin; microtubules; dorsal root ganglia; neuronal cell bodies

Introduction

Microtubule targeted agents (MTAs) are commonly used to treat many types of cancer. MTAs are thought to combat tumor growth by altering the growing and shortening dynamics of microtubules (Giannakakou et al. 2002; Jordan and Wilson 2004). Properly regulated microtubule dynamics are essential for intracellular transport mechanisms and cellular architecture. Disruption of these essential functions can lead to deleterious effects and even cell death (Argyriou et al. 2012; Fehrenbacher 2015; Field et al. 2014; Jordan and Wilson 2004; Poruchynsky et al. 2015).

MTAs are generally delivered to patients systemically, exposing both tumor and non-tumor tissues to the chemical assault, which can lead to serious side effects including chemotherapy-induced peripheral neuropathy (CIPN) (Argyriou et al. 2012; Argyriou et al. 2014; Carlson and Ocean 2011; Grisold et al. 2012). Though variable, approximately 30-40% of chemotherapy patients experience at least some CIPN symptoms including pain, hypersensitivity to pressure and hot or cold temperatures, tingling, burning sensations, numbness and/or loss of deep tendon reflexes. These symptoms often begin in the distal extremities (*i.e.*, fingertips and toes) and progress proximally up the arms and legs, suggesting that the longest nerves are most vulnerable (Argyriou et al. 2012; Carlson and Ocean 2011; Fehrenbacher 2015; Grisold et al. 2012; Windebank and Grisold 2008). CIPN symptoms can be sufficiently severe as to necessitate dose reduction or treatment cessation, thereby being a significant impediment to favorable outcomes and quality of life (Argyriou et al. 2014; Carlson and Ocean 2011; Windebank and Grisold 2008).

The onset, rate of progression, severity and reversibility of CIPN symptoms vary greatly among different MTA treatments (Argyriou et al. 2012; Carlson and Ocean 2011; Grisold et al. 2012). Different MTAs also vary in the frequencies at which they induce severe peripheral neuropathy. For instance, patients treated with paclitaxel tend to exhibit a higher frequency of severe CIPN than do patients treated with eribulin (Argyriou et al. 2012; Gradishar 2011).

While all MTAs affect microtubule dynamics, the different classes of MTAs vary in their mechanisms of action. For example, the taxanes (e.g. paclitaxel) bind the inner surface of the microtubule lattice along its entire length (Jordan and Wilson 2004) and promote microtubule (MT) stability and suppression of MT shortening events, leading to net MT polymerization (Derry et al. 1995; Jordan et al. 2005). In contrast, eribulin binds selectively to the plus ends of MTs as well as to soluble tubulin subunits, preventing the addition of new subunits without affecting normal subunit loss and therefore lead to net MT depolymerization (Jordan et al. 2005; Smith et al. 2010). Thus, although these two MTAs exhibit different molecular mechanisms of action, both alter the normal patterns of microtubule dynamics and compromise normal MT activities (Bunker et al. 2004; Jordan

and Wilson 2004). These observations have led us to hypothesize that the different mechanisms of action for different MTAs may underlie the variability in MTA-induced development, severity, and persistence of CIPN symptoms.

Given their importance, it is not surprising that cells invest considerable effort to properly regulate their microtubule dynamics using a variety of molecular mechanisms, including post-translational modifications, binding of microtubule associated proteins (MAPs) and altered tubulin isotype expression patterns. Alone or in combination, these mechanisms can provide highly tunable regulatory power (Bhattacharya et al. 2011; Janke and Bulinski 2011; Lu and Luduena 1993; Savage et al. 1989; Song and Brady 2015). For example, acetylation of α-tubulin at lys-40 is a well-established marker of microtubule stability and recent work suggests that acetylation may itself actively confer MT stability (Dompierre et al. 2007; Godena et al. 2014; Janke and Bulinski 2011). Additionally, a number of MAPs bind to microtubules and regulate their dynamics. For example, microtubule end binding proteins EB1 and EB3 bind selectively to the growing plus ends of microtubules, facilitating MT polymerization, directional cues and cross-links to actin filaments (Akhmanova and Steinmetz 2015; Maurer et al. 2012) (Geraldo et al. 2008; Gu et al. 2006; Jaworski et al. 2009). Finally, cells can regulate the relative expression levels of different tubulin isotypes to modify protofilament number or more subtle microtubule properties as well as relative susceptibility to stabilizing or destabilizing molecules (Bhattacharya et al. 2011; Lu and Luduena 1993; Savage et al. 1989). The number and diversity of regulatory mechanisms support the notion of a tightly regulated microtubule network that is essential for survival and function of both dividing and post-mitotic cells. We have previously proposed that dysregulation of microtubule dynamics outside of a tolerable range can lead to severe deleterious effects for cells, including post-mitotic neurons (Bunker et al. 2004).

A commonly held hypothesis for MTA-mediated action in post-mitotic neurons proposes that MTAs disrupt microtubule-based fast axonal transport, leading to deleterious downstream changes in axon biochemistry and subsequent neurodegeneration (Morfini et al. 2009). In vitro experiments in squid axoplasm, SKNSH neuroblastoma cell culture, and in vivo ligation models have all demonstrated that paclitaxel slows microtubule-based anterograde transport of organelles and proteins more potently than does eribulin (Lapointe et al. 2013) (Smith et al. 2016).

Recently, we have examined the morphological and microtubule-based biochemical effects of paclitaxel and eribulin upon sciatic nerve axons in a two-week, maximum tolerated dose (MTD) mouse model of CIPN, a dosing strategy chosen to reflect current standard clinical practice (Benbow et al. 2016). While both paclitaxel and eribulin exerted notable effects upon axon morphology and biochemistry, paclitaxel was markedly more disruptive of myelin morphology and induced more frequent signs of neurodegeneration than did eribulin treatment, consistent with recent work demonstrating paclitaxel's greater functional deficits in nerve conduction velocity and signal amplitude versus eribulin (Wozniak et al. 2011). Treatment with either MTA also induced altered biochemistry of sciatic nerve axonal microtubules and microtubule-associated proteins. Remarkably, despite the fact that eribulin is traditionally viewed as a microtubule destabilizing drug based on short term in vitro and cell culture exposure experiments, long-term treatment of mice with eribulin increased the

abundance of axonal proteins indicative of microtubule growth and stability significantly more than did treatment with paclitaxel (Benbow et al. 2016). These observations suggested long-term cellular response mechanisms through which neurons may compensate for at least some of the deleterious effects of drugs upon their microtubule networks (Benbow et al. 2016).

The cell bodies of long sensory axons of the sciatic nerve are located in the dorsal root ganglia (DRG), located just outside of the spinal cord. Although they are different compartments of the same cells, the long axons and cell bodies are highly specialized and distinct from one another in terms of structure and function. For example, axonal microtubules are more stable/less dynamic than cell body microtubules (Janke 2014; Song and Brady 2015). It follows that cell bodies and axons may respond differently to stress and stimuli (*e.g.* chemotherapeutic assault). To test this notion, we conducted a detailed morphological and biochemical examination of MTA effects on DRG neuronal cell bodies to complement and extend our previous work. Overall, the effects of both drugs were much less marked in the cell bodies than in their axons. However, paclitaxel induced greater levels of neuronal stress and potentially deleterious changes to cell body biochemistry than did eribulin, which exhibited only minimal effects. Taken together, DRG neuronal cell bodies and their axons contain functionally distinct microtubule networks that exhibit unique biochemical responses to different MTA treatments. We hypothesize that the distinct mechanistic actions of paclitaxel and eribulin elicit different cellular and molecular responses, which may underlie the variability seen in the initiation, progression, persistence and recovery from neuropathic symptoms.

Materials and Methods

Antibodies

Primary antibodies used in this study include: Anti-βIII tubulin (abcam, ab107216, 1:1000 dilution)(Rinkevich et al. 2014)), anti-ATF3 (C-19), (Santa Cruz SC-188, 1:1000 dilution, (Carozzi et al. 2013)), anti-α-tubulin (Millipore, 04-1117, 1:100 dilution (Zhang et al. 2011)), anti-acetylated tubulin(Cell Signal, 5335, 1:800 dilution, (Creppe et al. 2009)), anti-EB1 (Millipore, AB6057, 1:500 dilution, (Vitre et al. 2008)), anti-EB3 (Santa Cruz, SC-101475, 1:200 dilution, (Levy et al. 1994)) and anti-phosphoneurofilament (Covance, SMI-31R, 1:2000 dilution, (Choi et al. 2008)). Secondary antibodies used in this study included: Cy2-conjugated donkey anti-rabbit (711-225-152), Cy2-conjugated donkey anti rat (712-225-153), Cy3-conjugated donkey anti-chicken (703-165-155), and Cy5-conjugated donkey anti-mouse (715-175-151) (all purchased from Jackson Immunoresearch, (West Grove, PA)).

Drugs

Eribulin mesylate (E7389, previously ER-086526 and NSC-707389) synthesized at Eisai Research Institute and stored at -80 degrees in the dark) was dissolved in 100% anhydrous DMSO (Sigma-Aldrich, St. Louis, MO) to produce a 10 mg/mL stock solution, which was separated into aliquots and stored at −80°C until day of administration. Each administration day the stock solution was thawed and diluted with saline to a final concentration of 0.125

mg/mL in 2.5% DMSO/97.5% saline and administered in a 10 mL/kg volume. Paclitaxel (purchased from LC Laboratories, Woburn, MA and stored at -20 degrees C, in the dark) was dissolved in ethanol (100%) at 10% of final volume. An equal volume of cremophor (10% of final volume) was then added and the mixture re-vortexed for about 10 min. Immediately prior to injection, ice-cold saline was added to final volume (as 80% of final) and the solution was maintained on ice during dosing. Dosing solutions of 3 mg/mL were made fresh daily and administered in a 10 mL/kg volume.

Animal Procedures

Female BALB/c mice (approximately 7-8 weeks old at onset of dosing) were obtained from Harlan Laboratories (Indianapolis, IN) and maintained with free access to water and a standardized synthetic diet (Harlan Teklab). Animal housing and procedure room temperature and humidity were maintained at 20 + 2°C and 55 + 10% respectively. Artificial lighting provided a 12h light/12h dark cycle (light 7am-7pm). All experimental protocols were approved by the Institutional Animal Care and Use Committee of Johns Hopkins and adhered to all of the applicable institutional and governmental guidelines for the humane treatment of laboratory animals.

Mice were treated with a previously determined 6 dose MTD regimen, administered intravenously every other day for 2 weeks with a 2 day rest period between weekly cycles (Wozniak et al 2011). MTD was defined as the maximal dose of eribulin mesylate or paclitaxel administered at which no more than one animal in the treatment group died spontaneously. In addition, this was the maximal dose tested at which no mice in the dose group required euthanasia due to >20% individual weight loss, showing overt clinical signs of distress or inability to eat and/or drink. The MTD dose, when administered IV 6 times on the above schedule, was determined to be 1.25 mg/kg (~3.75 mg/m^2) for eribulin and 30 mg/kg (90 mg/m^2) for paclitaxel. The maximum tolerated dose model was chosen to reflect standard clinical practice in which physicians frequently dose human patients. The current recommended dosing strategy for human patients for eribulin mesylate is 1.4mg/m^2 delivered by infusion over 2 to 5 minutes on days 1 and 8 of a 21-day cycle, whereas higher doses of paclitaxel (135- or 175 mg/m^2 every there weeks) are commonly recommended (Bristol-Myers-Squibb 2011; Eisai-Inc. 2016). Additionally, the comparison of such different doses is supported by preclinical cell culture and in vivo experiments demonstrating a similarly large difference in the two drugs' doses and overall cytotoxicity profile (Towle et al. 2001). These different doses highlight the fact that eribulin's potency (both anticancer efficacy and associated toxicities) occurs at significantly lower dose levels than those of paclitaxel. Xenograft doses of paclitaxel in Towle et al. (12.5-25 mg/kg or ~38-77 mg/m^2) were higher compared to eribulin (0.05-1.0mg/kg or ~0.15-3.0 mg/m^2) and demonstrated a range of efficacious anticancer doses that included the eribulin dose used in Cortes et al. 2012 in humans (1.4 mg/m^2). Indeed, this differential is reflected in the FDA-recommended clinical dosing levels of the two drugs for breast cancer 1.4mg/m^2 for eribulin mesylate versus 135-175 mg/m^2 for paclitaxel.

Twenty-four hours after receiving the last dose, animals from each treatment group underwent transcardial perfusion with paraformaldehyde 4% in 0.1 mM phosphate buffer,

pH 7.4, for 10-15 minutes, while under deep anaesthesia (10% chloral hydrate). L4-L5 Dorsal Root ganglia (DRG) and left and right sciatic nerves at mid-thigh were dissected out from these mice. The specimens were fixed by immersion in 4% paraformaldehyde.

Tissue Sectioning

Fixed, whole dorsal root ganglia were cryo-protected at 4°C overnight in 30% sucrose (weight/volume) dissolved in PBS (1.37 M NaCl, 27 mM KCl, 100 mM Na_2HPO_4, 18 mM KH_2PO_4) with 0.01% sodium azide. Tissue was embedded in Richard Allan Scientific Neg-50 frozen section medium (Thermo Scientific #6502) by freezing at -50°C. Sections were taken using a Microm HM560 cryostat (ThermoFisher Scientific, Waltham, MA) set to 16 μm thickness, and thaw-mounted onto charged glass slides (two sections per slide). Slides were allowed to dry overnight prior to storage at -80°C.

Fixed whole sciatic nerves were processed as described previously (Benbow et al. 2016). Briefly, sciatic nerves were embedded in 10% agarose (w/v) dissolved in 1X PBS with 0.01% sodium azide. Tissue was cross-sectioned distally to proximally in 100 μm sections using a Vibratome 1000 plus sectioning system. Sciatic nerve sections were collected in PBS and stored in 1X PBS with 0.01% sodium azide at 4°C until immunostaining.

Antibody Staining

Just prior to staining, DRG sections were thawed and dried. All blocking and antibody incubations and washes were performed at room temperature in stationary humid chambers. Sections were incubated in PBT blocking agent (1X PBS, 0.1 % TritonX-100, 1% BSA, 1% donkey serum) for 2 hours, then overnight in primary antibodies diluted in PBT blocking agent. Two sections from each of the four treatment groups (vehicle paclitaxel, paclitaxel, vehicle eribulin and eribulin) were stained simultaneously with the same antibody solution. Stained slides were mounted using ProLong Gold Antifade mounting media with DAPI (ThermoFisher Scientific). Slides were stored at 4°C prior to and after imaging.

Sciatic nerve sections were grouped so that one section from each treatment condition was stained with the same antibody solution. Antibodies were diluted to the same concentrations used in DRG staining in PBT block. Sections were incubated free-floating, at 4°C for 7 days to promote antibody penetration, washed three times in PBT (10 minutes each wash) and then incubated in secondary antibody for two days. Sections were then washed three times, ten minutes each, as in the previous wash step and mounted onto glass slides with ProLong Gold Antifade mounting media with DAPI (ThermoFisher Scientific). Slides were stored at 4°C until imaging.

Image acquisition

Images were collected on an Olympus Fluoview 1000 spectral confocal microscope equipped with 405, 488, 559 and 635 nm laser lines and photomultiplier tube detectors. Identical exposure settings (exposure time, laser intensity, offset and gain) were used for sample groups treated with the same antibody solution by first identifying the brightest fluorescing sample within the treatment set. Each sample was imaged in 0.5 μm steps

through 16 μm sample depth using sequential laser scanning with an Olympus PLANAPOSC 60× (1.40 NA) high refractive index oil immersion objective.

Image analysis

Image analysis was performed using Imaris Software version 7.5.2 (Bitplane, Zurich, Switzerland). Image Z-stacks were imported into Imaris software and rendered into three-dimensional maximum-intensity projections for further analysis. All analyses were completed using three-dimensional projections to ensure retention and evenly account for fluorescence data of individual planes. Images acquired from sections stained with the same antibody solution, using the same exposure settings, were grouped as “image sets” for analysis (each group contained one section from each treatment condition; Figure S1) and received the same analysis parameters. For DRG analyses, regions of interest containing DRG cell bodies were manually selected to exclude tissue containing predominantly axons (Figure S2). To assess relative levels of neuronal injury, Imaris software was used to quantitate the total number of nuclei per 10^4 μm^2 area of DRG tissue. The percent of ATF3 positive neuronal nuclei were counted manually. In order to quantify relative changes in fluorescence of proteins of interest (α-tubulin, acetylated-tubulin, end binding protein 1 (EB1) and end binding protein 3 (EB3)) within DRG neurons, we further restricted the manually defined non-axonal DRG region, using anti-βIII-tubulin antibody staining to identify and mask neuronal cell bodies and identify neurons from other cell types present in the DRG. The mean fluorescent signal of a given protein of interest was calculated for a given section and three dimensional region of βIII-tubulin positive (neuronal) tissue, with each βIII-tubulin positive volumetric pixel (voxel) contributing a fluorescence value for the protein in question. The normalization procedure is illustrated in Figure S3. Raw fluorescence values for the protein of interest within βIII positive regions were collected and averaged over a given section producing the “treatment-mean”. Treatment-means were normalized by dividing the section-mean of one treatment by the sum of section-means of that image group. This method was employed to retain the natural variability within vehicle treatment conditions. This was the same methodology used previously (Benbow et al. 2016)

Statistical Analysis

One-way ANOVAs with post-hoc Tukey's tests were employed to test the statistical significance between differences in the means of treatment groups in all instances unless otherwise noted (*p<0.05, **p<0.01, ***p<0.001). In cases in which the variances between conditions were statistically different, Bonferroni corrected Student's T-Tests for multiple comparisons were employed (*p<0.0167, **<p0.003, ***p<0.003). N=5 for all DRG analyses except EB1, which was N=4. Sciatic nerve tissue from three mice for each treatment condition was analyzed for relative levels of β-III tubulin (N=3). Error bars within graphs represent the standard error of the mean (SEM).

Results

Paclitaxel but not eribulin increases the abundance of ATF3 positive nuclei

Activating transcription factor 3 (ATF3) is commonly used as a marker for neuronal injury and stress (Carozzi et al. 2013; Tsujino et al. 2000). The percent of ATF3 positive nuclei in

the DRG of two-week paclitaxel, eribulin or vehicle treated mice was quantitated by counting the number of ATF3 positive neuronal nuclei as compared to the total number of neuronal nuclei present. The mean percent of ATF3 positive neuronal nuclei increased significantly in DRG tissue from paclitaxel but not eribulin treated mice compared to their respective vehicle controls, (Figures 1A and 1B). Paclitaxel treated DRG contained an average of 49.8 ± SEM 8.7% of neuronal nuclei expressing ATF3, whereas very few ATF3 positive nuclei were seen in the tissue from mice treated with the vehicle for paclitaxel (0.3 ± 0.3%, $p<0.001$). Eribulin treatment led to a small but not statistically significant ($p>0.05$) increase in ATF3 positive nuclei (13.9 ± 3.1%) relative to the vehicle for eribulin. The difference between paclitaxel treatment and eribulin treatment was statistically significant ($p<0.01$)

As an increase in non-neuronal cells within nerve tissue can also indicate nerve injury (Janes et al. 2014; Peters et al. 2007a; Peters et al. 2007b; Rotshenker 2011; Zhang et al. 2016), we sought to assess whether DRG would exhibit an increase in non-neuronal cells after a two week MTD drug treatment. Since DRG neurons are post-mitotic in adult mice, any increase in the number of DRG nuclei would be the result of an increased number of non-neuronal cells. Therefore, we quantified the total number of nuclei present per 10^4 μm^2 DRG tissue, as indicated by DAPI staining. Neither paclitaxel or eribulin or their vehicle treatments led to any significant change in the mean number of nuclei per 10^4 μm^2 area of DRG tissue, with observed means of 105 ± SEM 4.3, 108.3 ± 7.8, 113.4 ± 8.7 and 118 ± 3.8 nuclei for vehicle paclitaxel, paclitaxel, vehicle eribulin, and eribulin respectively (Figures 1B and 1C).

Paclitaxel but not eribulin alters microtubule biochemistry in DRG neuronal cell bodies

We next examined changes to the tubulin composition in the DRG between paclitaxel, eribulin and vehicle treated mice, using anti-α-tubulin, anti-βIII-tubulin and anti-acetylated-tubulin antibodies. Total tubulin content, as indicated by anti-α-tubulin fluorescence, was not significantly different in DRG neuronal cell bodies treated with either drug relative to its vehicle (Figures 2A and 2B). Mean fluorescent signals observed were 22.5 ± SEM 2.3 arbitrary fluorescence units (A.U.s) for vehicle paclitaxel, 22.8 ± 2.1 for paclitaxel, 26.1 ± 1.0 for vehicle eribulin and 28.7 ± 1.7 for eribulin ($p > 0.05$). In contrast, the abundance of βIII-tubulin increased approximately 1.3-fold from a mean of 21.6 ± 0.6 A.U.s observed in the DRG neuronal cell bodies from vehicle paclitaxel treated mice to 28.9 ± 1.0 observed in the DRG neuronal cell bodies from paclitaxel treated mice ($p< 0.001$, when paclitaxel is compared to its vehicle, and $p < 0.05$ when paclitaxel is compared to eribulin, Figure 3A). These data are consistent with the paclitaxel-mediated induction of βIII-tubulin in cultured cancer cell lines (Kamath et al. 2005; Ranganathan et al. 1996). In contrast, eribulin treatment did not induce a significant change of βIII-tubulin levels from the vehicle control condition (24.0 ± 0.7 compared to 25.5 ± 0.1, respectively ($p > 0.05$, Figure 3A and 3B).

As changes to levels of β-III tubulin in sciatic nerve in response to chemotherapy treatment were not explored in our previous study, we examined sciatic nerve tissue immunostained for β-III tubulin within the current set of experiments to enable their comparison. Surprisingly, our results demonstrated that both paclitaxel and eribulin treatment modestly reduced axonal β-III tubulin levels within sciatic nerve tissue (Figure 3C and 3D). The mean

fluorescent signals from axonal βIII-tubulin in paclitaxel and eribulin treated mice (23.5 ± SEM 0.7 and 21.6 ± 0.8, respectively) were statistically different compared to the mean levels of axonal βIII-tubulin signal in mice treated with their respective vehicles (29.0 ± 0.4 for vehicle paclitaxel; $p < 0.01$, 25.9 ± 1.0 for vehicle eribulin, $p < 0.05$, Figure 3C and 3D). There was no statistically significant difference between paclitaxel and eribulin means ($p > 0.05$), indicating a similar degree of effect with each drug. While both drugs altered levels of axonal βIII-tubulin, there was no statistical difference in mean axonal βIII-tubulin levels between paclitaxel and eribulin treatments.

Acetylation of α-tubulin at lysine-40 is a well-established marker for microtubule stability, as acetylation has been observed most commonly in long-lived microtubules (Black and Keyser 1987; Janke and Bulinski 2011; Webster and Borisy 1989). We used anti-acetylated-tubulin immuno-staining to assess the relative levels of acetylated tubulin as an indication of the stability of the microtubule network within the cell bodies of sciatic neurons. Paclitaxel treatment significantly increased the relative level of acetylated tubulin 1.9-fold from 21.1 ± SEM 2.2 in the DRG neurons from the mice treated with the paclitaxel vehicle control to a mean fluorescence of 41.7 ± 3.3 observed in the DRG neurons from paclitaxel treated mice ($p<0.001$, Figure 4A and 4B). Eribulin on the other hand, did not alter the levels of acetylated tubulin significantly as compared to treatment with its vehicle control. The mean level of acetylated tubulin for paclitaxel treatment was also statistically different from the mean level of acetylated tubulin observed in eribulin treatment (20.7 ± 2.4 A.U.s, $p<0.001$, Figure 4A).

Paclitaxel but not eribulin increases the level of EB1, but not EB3, in DRG neuronal cell bodies

As a marker for growing microtubules, we next assessed the abundance of the microtubule end binding proteins EB1 and EB3. DRG from paclitaxel treated mice exhibited a 2.0 fold difference in mean fluorescent signal of 35.4 ± SEM 0.8 as compared to the vehicle control for paclitaxel (17.5 ± SEM 1.7, $p < 0.001$, Figure 5A and 5B). In contrast, eribulin treatment did not result in a statistically significant change in EB1 signal as compared to its vehicle control (26.1 ± 1.9 and 21.1 ± 1.8, respectively, $p > 0.05$). The increase observed with paclitaxel was also statistically different from the signal seen after eribulin treatment ($p < 0.01$).

On the other hand, EB3 immunostaining revealed no changes in EB3 abundance as a result of either MTA treatment ($p>0.05$, Figure 5C and 5D) relative to their corresponding vehicle controls. DRG tissue from paclitaxel treated mice showed a mean fluorescent signal of 24.8 ± SEM 1.7, Eribulin demonstrated a mean signal of 25.5 ± 2.6 whereas the vehicle for paclitaxel and the vehicle for eribulin demonstrated means of 21.6 ± 1.8 and 28.3 ± 2.1, respectively.

Discussion

In an effort to better understand the underlying mechanisms of CIPN, we sought to investigate MTA-induced effects upon the microtubule network of sensory nerve cells. Our specific goal was to test the hypothesis that MTAs possessing different mechanisms of

action differentially affect neuronal cell bodies and axons of the sciatic nerve. We have examined MTA effects on sciatic nerve axons (Benbow et al. 2016) and their DRG cell bodies (here), allowing compartmental comparison of effects and providing novel insights to MTA-induced peripheral neuropathy.

Paclitaxel induces greater neuronal stress than eribulin, correlating with more severe morphological disruptions

Our previous work examining two-week maximum tolerated dose effects of MTAs on sciatic nerve axons revealed that paclitaxel induced nerve fiber collapses with greater frequency than did eribulin (Benbow et al. 2016). This led us to ask in the current work if MTA-induced effects of neuronal injury or stress would be evident in the corresponding DRG cell bodies after similar drug treatment. Using ATF3 expression as a marker for neuronal stress (Carozzi et al. 2013; Tsujino et al. 2000), the data demonstrate that paclitaxel but not eribulin induces a significant increase in the percentage of neuronal nuclei exhibiting ATF3 expression, suggesting neurons experience greater stress upon paclitaxel treatment compared to eribulin treatment.

Paclitaxel and eribulin differentially affect peripheral neuron cell bodies and axons

As noted above, paclitaxel induces a significantly higher frequency of severe CIPN than does eribulin. Consistent with this observation, paclitaxel induces more frequent morphological abnormalities and signs of neurodegeneration than does eribulin in our preclinical two-week MTD experiments on mouse sciatic nerves (Benbow et al. 2016). Biochemically, both paclitaxel and eribulin induced large increases in total tubulin abundance and tubulin acetylation, with eribulin mediating even larger inductions than paclitaxel (summarized in Table 1). Importantly, large increases in tubulin concentration and acetylated tubulin abundance are both likely to promote microtubule growth and stabilization. Given that axons require a relatively stable microtubule network to conduct axonal transport and to maintain morphological stability, we hypothesized that the stronger eribulin mediated increase in the axonal microtubule network might counter the deleterious effects of eribulin more effectively than paclitaxel's stabilizing effects might counter its deleterious effects.

In the current work, we have extended our earlier axonal work by comparing the effects of paclitaxel and eribulin in the dorsal root ganglia cells that are the neuronal cell bodies of the sciatic nerve sensory axons. Many of the biochemical effects of the two drugs were quite different than observed in the axons. Neither drug affected total tubulin levels, although paclitaxel induced a slight increase in the levels of βIII tubulin (Figures 2 and 3, Table 1). Paclitaxel also increased the level of acetylated tubulin ~2 fold, whereas eribulin had no effect (Figure 4, Table 1). Similarly, paclitaxel treatment induced the levels of EB1 by ~2 fold, whereas eribulin treatment had no significant effect (Figures 4 and 5, Table 1). Thus, paclitaxel but not eribulin induces both biochemical changes and neuronal stress upon cell bodies. Further, paclitaxel affects tubulin biochemistry in a manner suggesting increased microtubule stabilization, although this effect is quantitatively much smaller than that observed in the axons. On the other hand, eribulin had essentially no detectable

morphological or biochemical effects in the cell bodies, again in contrast to its marked effects in axons.

Regionally specific effects of MTAs may underlie the development of CIPN

Peripheral sensory nerve axons can span enormous distances and possess multiple distinct regions with distinct functions. For example, these cells receive signals at their distal axon terminals in the periphery, then must propagate the signal along the entire length of their peripheral axon branch, bypassing the cell body and eventually relaying the signal along the central branch axon to the next cell in the circuit in the spinal cord. Consistent with the notion of region-specific functions, the microtubule network differs markedly with respect to tubulin isotype composition, tubulin post-translational modification and association with various microtubule associated proteins, thereby creating regionally and functionally distinct microtubule networks (Gundersen et al. 1987; Janke and Bulinski 2011; Song and Brady 2015). For example, axonal microtubules are enriched in acetylated and detyrosinated tubulin, indicating a high degree of stability, whereas microtubules in neuronal cell bodies have far lower concentrations of these tubulin modifications suggesting greater dynamicity (Janke and Kneussel 2010; Song and Brady 2015). This translates into distinct functionalities as axons require stable microtubules to mediate axonal transport over long distances, while functions in the cell body necessitate a more dynamic cytoskeletal network. Based on these observations, we predict that different MTAs may differentially affect microtubule action within a cell based on their regionally and functionally defined properties. Biochemically, both paclitaxel and eribulin treatment induced large increases in total tubulin abundance and tubulin acetylation in axons, and the eribulin mediated inductions were even larger than the paclitaxel inductions. These increases in tubulin and acetylated tubulin abundance are both likely to promote microtubule growth and stabilization. Given that axons require a relatively stable microtubule network to conduct axonal transport and to maintain morphological stability, we hypothesized that the more robust eribulin-mediated increase in the axonal microtubule network might serve to promote axonal transport and maintain axonal morphology. In contrast, microtubules in cell bodies are relatively dynamic (*i.e.*, less stable) (Janke 2014; Song and Brady 2015). The suggestion here that paclitaxel but not eribulin promotes increased microtubule stability in cell bodies that require more dynamic and less stable microtubules together with greater neuronal stress as indicated by ATF3 expression lead to the model that these actions of paclitaxel may be detrimental. Taken together with our earlier work (Benbow et al., 2016), we suggest that paclitaxel deleteriously alters microtubule biochemistry in both cell bodies and axons and speculate that these changes in microtubule biochemistry may contribute to the differential frequency of severe CIPN observed in clinics. Functional studies will be necessary to assess the validity of this model.

MTA exposure and CIPN induction

Another important issue to consider with respect to the differential induction of severe CIPN by paclitaxel versus eribulin is the possibility that the two drugs are taken up differentially by peripheral sensory neurons. In other words, might the apparent reduction in eribulin-mediated neuropathic events be the result of reduced exposure of peripheral neurons to eribulin as compared to paclitaxel? In this regard, recent work demonstrates that eribulin

actually has greater penetration and retention in dorsal root ganglia and axons of peripheral neurons than does paclitaxel (Wozniak et al. 2016).

Summary

Taken together with our earlier work (Benbow et al. 2016), we have shown that eribulin-induced effects are localized to axons, leaving the microtubule network within cell bodies generally unperturbed. In contrast, paclitaxel has significant effects in both DRG neuronal nuclei and axons. Previously, we had hypothesized that the effects observed with eribulin treatment in sciatic nerve axons ultimately led to an advantageous strengthening of the microtubule network within axons. We now additionally hypothesize that eribulin results in less severe microtubule network alteration in the neuronal cell bodies in the DRGs that are connected to the sciatic nerve axons than does paclitaxel, which may also contribute to differential induction of CIPN. Ongoing investigations aim to test this hypothesis mechanistically in in vitro, cell culture and animal models.

Supplementary Material

Refer to Web version on PubMed Central for supplementary material.

Acknowledgments

We are grateful to Nichole LaPointe, Brett Cook, Benjamin Reese, Patrick Keeley, Jennifer Smith and Mary Raven for valuable discussions and to Benjamin Reese for sharing equipment with us. We also acknowledge the use of instruments in the NRI-MCDB Microscopy Facility at UCSB (supported in part by the Office of The Director, National Institutes of Health of the NIH under Award # S10OD010610). This work was supported by grants from EISAI (to SCF, BSS, MAJ and LW) and the NIH/NCI (R01CA161056) to BSS.

References

Akhmanova A, Steinmetz MO. Control of microtubule organization and dynamics: two ends in the limelight. Nat Rev Mol Cell Biol. 2015; 16:711–726. DOI: 10.1038/nrm4084 [PubMed: 26562752]

Argyriou AA, Bruna J, Marmiroli P, Cavaletti G. Chemotherapy-induced peripheral neurotoxicity (CIPN): an update. Crit Rev Oncol Hematol. 2012; 82:51–77. DOI: 10.1016/j.critrevonc.2011.04.012 [PubMed: 21908200]

Argyriou AA, Kyritsis AP, Makatsoris T, Kalofonos HP. Chemotherapy-induced peripheral neuropathy in adults: a comprehensive update of the literature. Cancer Manag Res. 2014; 6:135–147. DOI: 10.2147/cmar.s44261 [PubMed: 24672257]

Benbow SJ, Cook BM, Reifert J, Wozniak KM, Slusher BS, Littlefield BA, Wilson L, Jordan MA, Feinstein SC. Effects of Paclitaxel and Eribulin in Mouse Sciatic Nerve: A Microtubule-Based Rationale for the Differential Induction of Chemotherapy-Induced Peripheral Neuropathy. Neurotox Res. 2016; 29:299–313. DOI: 10.1007/s12640-015-9580-6 [PubMed: 26659667]

Bhattacharya R, Yang H, Cabral F. Class V beta-tubulin alters dynamic instability and stimulates microtubule detachment from centrosomes. Mol Biol Cell. 2011; 22:1025–1034. DOI: 10.1091/mbc.E10-10-0822 [PubMed: 21289088]

Black MM, Keyser P. Acetylation of alpha-tubulin in cultured neurons and the induction of alpha-tubulin acetylation in PC12 cells by treatment with nerve growth factor. J Neurosci. 1987; 7:1833–1842. [PubMed: 3598651]

Bristol-Myers-Squibb. Taxol (paclitaxel) injection. Princeton; NJ: 2011. Package Insert

Bunker JM, Wilson L, Jordan MA, Feinstein SC. Modulation of microtubule dynamics by tau in living cells: implications for development and neurodegeneration. Mol Biol Cell. 2004; 15:2720–2728. DOI: 10.1091/mbc.E04-01-0062 [PubMed: 15020716]

Carlson K, Ocean AJ. Peripheral neuropathy with microtubule-targeting agents: occurrence and management approach. Clin Breast Cancer. 2011; 11:73–81. DOI: 10.1016/j.clbc.2011.03.006 [PubMed: 21569993]

Carozzi VA, Renn CL, Bardini M, Fazio G, Chiorazzi A, Meregalli C, Oggioni N, Shanks K, Quartu M, Serra MP, Sala B, Cavaletti G, Dorsey SG. Bortezomib-induced painful peripheral neuropathy: an electrophysiological, behavioral, morphological and mechanistic study in the mouse. PLoS One. 2013; 8:e72995.doi: 10.1371/journal.pone.0072995 [PubMed: 24069168]

Choi YJ, Di Nardo A, Kramvis I, Meikle L, Kwiatkowski DJ, Sahin M, He X. Tuberous sclerosis complex proteins control axon formation. Genes Dev. 2008; 22:2485–2495. [PubMed: 18794346]

Creppe C, Malinouskaya L, Volvert ML, Gillard M, Close P, Malaise O, Laguesse S, Cornez I, Rahmouni S, Ormenese S, Belachew S, Malgrange B, Chapelle JP, Siebenlist U, Moonen G, Chariot A, Nguyen L. Elongator controls the migration and differentiation of cortical neurons through acetylation of alpha-tubulin. Cell. 2009; 136:551–564. DOI: 10.1016/j.cell.2008.11.043 [PubMed: 19185337]

Derry WB, Wilson L, Jordan MA. Substoichiometric binding of taxol suppresses microtubule dynamics. Biochemistry. 1995; 34:2203–2211. [PubMed: 7857932]

Dompierre JP, Godin JD, Charrin BC, Cordelieres FP, King SJ, Humbert S, Saudou F. Histone deacetylase 6 inhibition compensates for the transport deficit in Huntington's disease by increasing tubulin acetylation. J Neurosci. 2007; 27:3571–3583. DOI: 10.1523/jneurosci.0037-07.2007 [PubMed: 17392473]

Eisai-Inc. Halaven [Package insert] Highlights of Prescribing Information. Woodcliff Lake; NJ: 2016.

Fehrenbacher JC. Chemotherapy-induced peripheral neuropathy. Prog Mol Biol Transl Sci. 2015; 131:471–508. DOI: 10.1016/bs.pmbts.2014.12.002 [PubMed: 25744683]

Field JJ, Kanakkanthara A, Miller JH. Microtubule-targeting agents are clinically successful due to both mitotic and interphase impairment of microtubule function. Bioorg Med Chem. 2014; 22:5050–5059. DOI: 10.1016/j.bmc.2014.02.035 [PubMed: 24650703]

Geraldo S, Khanzada UK, Parsons M, Chilton JK, Gordon-Weeks PR. Targeting of the F-actin-binding protein drebrin by the microtubule plus-tip protein EB3 is required for neuritogenesis. Nat Cell Biol. 2008; 10:1181–1189. DOI: 10.1038/ncb1778 [PubMed: 18806788]

Giannakakou P, Nakano M, Nicolaou KC, O'Brate A, Yu J, Blagosklonny MV, Greber UF, Fojo T. Enhanced microtubule-dependent trafficking and p53 nuclear accumulation by suppression of microtubule dynamics. Proc Natl Acad Sci U S A. 2002; 99:10855–10860. DOI: 10.1073/pnas.132275599 [PubMed: 12145320]

Godena VK, Brookes-Hocking N, Moller A, Shaw G, Oswald M, Sancho RM, Miller CC, Whitworth AJ, De Vos KJ. Increasing microtubule acetylation rescues axonal transport and locomotor deficits caused by LRRK2 Roc-COR domain mutations. Nat Commun. 2014; 5:5245.doi: 10.1038/ncomms6245 [PubMed: 25316291]

Gradishar WJ. The place for eribulin in the treatment of metastatic breast cancer. Curr Oncol Rep. 2011; 13:11–16. DOI: 10.1007/s11912-010-0145-9 [PubMed: 21104168]

Grisold W, Cavaletti G, Windebank AJ. Peripheral neuropathies from chemotherapeutics and targeted agents: diagnosis, treatment, and prevention. Neuro Oncol. 2012; 14(4):iv45–54. DOI: 10.1093/neuonc/nos203 [PubMed: 23095830]

Gu C, Zhou W, Puthenveedu MA, Xu M, Jan YN, Jan LY. The microtubule plus-end tracking protein EB1 is required for Kv1 voltage-gated K+ channel axonal targeting. Neuron. 2006; 52:803–816. DOI: 10.1016/j.neuron.2006.10.022 [PubMed: 17145502]

Gundersen GG, Khawaja S, Bulinski JC. Postpolymerization detyrosination of alpha-tubulin: a mechanism for subcellular differentiation of microtubules. J Cell Biol. 1987; 105:251–264. [PubMed: 2886509]

Janes K, Little JW, Li C, Bryant L, Chen C, Chen Z, Kamocki K, Doyle T, Snider A, Esposito E, Cuzzocrea S, Bieberich E, Obeid L, Petrache I, Nicol G, Neumann WL, Salvemini D. The development and maintenance of paclitaxel-induced neuropathic pain require activation of the sphingosine 1-phosphate receptor subtype 1. J Biol Chem. 2014; 289:21082–21097. DOI: 10.1074/jbc.M114.569574 [PubMed: 24876379]

Janke C. The tubulin code: molecular components, readout mechanisms, and functions. J Cell Biol. 2014; 206:461–472. DOI: 10.1083/jcb.201406055 [PubMed: 25135932]

Janke C, Bulinski JC. Post-translational regulation of the microtubule cytoskeleton: mechanisms and functions. Nat Rev Mol Cell Biol. 2011; 12:773–786. DOI: 10.1038/nrm3227 [PubMed: 22086369]

Janke C, Kneussel M. Tubulin post-translational modifications: encoding functions on the neuronal microtubule cytoskeleton. Trends Neurosci. 2010; 33:362–372. DOI: 10.1016/j.tins.2010.05.001 [PubMed: 20541813]

Jaworski J, Kapitein LC, Gouveia SM, Dortland BR, Wulf PS, Grigoriev I, Camera P, Spangler SA, Di Stefano P, Demmers J, Krugers H, Defilippi P, Akhmanova A, Hoogenraad CC. Dynamic microtubules regulate dendritic spine morphology and synaptic plasticity. Neuron. 2009; 61:85–100. DOI: 10.1016/j.neuron.2008.11.013 [PubMed: 19146815]

Jordan MA, Kamath K, Manna T, Okouneva T, Miller HP, Davis C, Littlefield BA, Wilson L. The primary antimitotic mechanism of action of the synthetic halichondrin E7389 is suppression of microtubule growth. Mol Cancer Ther. 2005; 4:1086–1095. DOI: 10.1158/1535-7163.mct-04-0345 [PubMed: 16020666]

Jordan MA, Wilson L. Microtubules as a target for anticancer drugs. Nat Rev Cancer. 2004; 4:253–265. DOI: 10.1038/nrc1317 [PubMed: 15057285]

Kamath K, Wilson L, Cabral F, Jordan MA. BetaIII-tubulin induces paclitaxel resistance in association with reduced effects on microtubule dynamic instability. J Biol Chem. 2005; 280:12902–12907. DOI: 10.1074/jbc.M414477200 [PubMed: 15695826]

Lapointe NE, Morfini G, Brady ST, Feinstein SC, Wilson L, Jordan M. Effects of eribulin, vincristine, paclitaxel and ixabepilone on fast axonal transport and kinesin-1 driven microtubule gliding: Implications for chemotherapy-induced peripheral neuropathy. Neurotoxicology. 2013; doi: 10.1016/j.neuro.2013.05.008

Levy DB, Smith KJ, Beazer-Barclay Y, Hamilton SR, Vogelstein B, Kinzler KW. Inactivation of both APC alleles in human and mouse tumors. Cancer Res. 1994; 54:5953–5958. [PubMed: 7954428]

Lu Q, Luduena RF. Removal of beta III isotype enhances taxol induced microtubule assembly. Cell Struct Funct. 1993; 18:173–182. [PubMed: 7902216]

Maurer SP, Fourniol FJ, Bohner G, Moores CA, Surrey T. EBs recognize a nucleotide-dependent structural cap at growing microtubule ends. Cell. 2012; 149:371–382. DOI: 10.1016/j.cell.2012.02.049 [PubMed: 22500803]

Morfini GA, Burns M, Binder LI, Kanaan NM, LaPointe N, Bosco DA, Brown RH Jr, Brown H, Tiwari A, Hayward L, Edgar J, Nave KA, Garberrn J, Atagi Y, Song Y, Pigino G, Brady ST. Axonal transport defects in neurodegenerative diseases. J Neurosci. 2009; 29:12776–12786. DOI: 10.1523/jneurosci.3463-09.2009 [PubMed: 19828789]

Peters CM, Jimenez-Andrade JM, Jonas BM, Sevcik MA, Koewler NJ, Ghilardi JR, Wong GY, Mantyh PW. Intravenous paclitaxel administration in the rat induces a peripheral sensory neuropathy characterized by macrophage infiltration and injury to sensory neurons and their supporting cells. Exp Neurol. 2007a; 203:42–54. DOI: 10.1016/j.expneurol.2006.07.022 [PubMed: 17005179]

Peters CM, Jimenez-Andrade JM, Kuskowski MA, Ghilardi JR, Mantyh PW. An evolving cellular pathology occurs in dorsal root ganglia, peripheral nerve and spinal cord following intravenous administration of paclitaxel in the rat. Brain Res. 2007b; 1168:46–59. DOI: 10.1016/j.brainres.2007.06.066 [PubMed: 17698044]

Poruchynsky MS, Komlodi-Pasztor E, Trostel S, Wilkerson J, Regairaz M, Pommier Y, Zhang X, Kumar Maity T, Robey R, Burotto M, Sackett D, Guha U, Fojo AT. Microtubule-targeting agents augment the toxicity of DNA-damaging agents by disrupting intracellular trafficking of DNA repair proteins. Proc Natl Acad Sci U S A. 2015; 112:1571–1576. DOI: 10.1073/pnas.1416418112 [PubMed: 25605897]

Ranganathan S, Dexter DW, Benetatos CA, Chapman AE, Tew KD, Hudes GR. Increase of beta(III)- and beta(IVa)-tubulin isotopes in human prostate carcinoma cells as a result of estramustine resistance. Cancer Res. 1996; 56:2584–2589. [PubMed: 8653701]

Rinkevich Y, Montoro DT, Muhonen E, Walmsley GG, Lo D, Hasegawa M, Januszyk M, Connolly AJ, Weissman IL, Longaker MT. Clonal analysis reveals nerve-dependent and independent roles on mammalian hind limb tissue maintenance and regeneration. Proc Natl Acad Sci U S A. 2014; 111:9846–9851. DOI: 10.1073/pnas.1410097111 [PubMed: 24958860]

Rotshenker S. Wallerian degeneration: the innate-immune response to traumatic nerve injury. J Neuroinflammation. 2011; 8:109.doi: 10.1186/1742-2094-8-109 [PubMed: 21878125]

Savage C, Hamelin M, Culotti JG, Coulson A, Albertson DG, Chalfie M. mec-7 is a beta-tubulin gene required for the production of 15-protofilament microtubules in Caenorhabditis elegans. Genes Dev. 1989; 3:870–881. [PubMed: 2744465]

Smith JA, Slusher BS, Wozniak KM, Farah MH, Smiyun G, Wilson L, Feinstein S, Jordan MA. Structural basis for induction of peripheral neuropathy by microtubule-targeting cancer drugs. Cancer Res. 2016; doi: 10.1158/0008-5472.can-15-3116

Smith JA, Wilson L, Azarenko O, Zhu X, Lewis BM, Littlefield BA, Jordan MA. Eribulin binds at microtubule ends to a single site on tubulin to suppress dynamic instability. Biochemistry. 2010; 49:1331–1337. DOI: 10.1021/bi901810u [PubMed: 20030375]

Song Y, Brady ST. Post-translational modifications of tubulin: pathways to functional diversity of microtubules. Trends Cell Biol. 2015; 25:125–136. DOI: 10.1016/j.tcb.2014.10.004 [PubMed: 25468068]

Towle MJ, Salvato KA, Budrow J, Wels BF, Kuznetsov G, Aalfs KK, Welsh S, Zheng W, Seletsky BM, Palme MH, Habgood GJ, Singer LA, Dipietro LV, Wang Y, Chen JJ, Quincy DA, Davis A, Yoshimatsu K, Kishi Y, Yu MJ, Littlefield BA. In vitro and in vivo anticancer activities of synthetic macrocyclic ketone analogues of halichondrin B. Cancer Res. 2001; 61:1013–1021. [PubMed: 11221827]

Tsujino H, Kondo E, Fukuoka T, Dai Y, Tokunaga A, Miki K, Yonenobu K, Ochi T, Noguchi K. Activating transcription factor 3 (ATF3) induction by axotomy in sensory and motoneurons: A novel neuronal marker of nerve injury. Mol Cell Neurosci. 2000; 15:170–182. DOI: 10.1006/mcne.1999.0814 [PubMed: 10673325]

Vitre B, Coquelle FM, Heichette C, Garnier C, Chretien D, Arnal I. EB1 regulates microtubule dynamics and tubulin sheet closure in vitro. Nat Cell Biol. 2008; 10:415–421. DOI: 10.1038/ncb1703 [PubMed: 18364701]

Webster DR, Borisy GG. Microtubules are acetylated in domains that turn over slowly. J Cell Sci. 1989; 92(Pt 1):57–65. [PubMed: 2674164]

Windebank AJ, Grisold W. Chemotherapy-induced neuropathy. J Peripher Nerv Syst. 2008; 13:27–46. DOI: 10.1111/j.1529-8027.2008.00156.x [PubMed: 18346229]

Wozniak KM, Nomoto K, Lapidus RG, Wu Y, Carozzi V, Cavaletti G, Hayakawa K, Hosokawa S, Towle MJ, Littlefield BA, Slusher BS. Comparison of neuropathy-inducing effects of eribulin mesylate, paclitaxel, and ixabepilone in mice. Cancer Res. 2011; 71:3952–3962. DOI: 10.1158/0008-5472.can-10-4184 [PubMed: 21498637]

Wozniak KM, Vornov JJ, Wu Y, Nomoto K, Littlefield BA, DesJardins C, Yu Y, Lai G, Reyderman L, Wong N, Slusher BS. Sustained Accumulation of Microtubule-Binding Chemotherapy Drugs in the Peripheral Nervous System: Correlations with Time Course and Neurotoxic Severity. Cancer Res. 2016; 76:3332–3339. DOI: 10.1158/0008-5472.can-15-2525 [PubMed: 27197173]

Zhang H, Li Y, de Carvalho-Barbosa M, Kavelaars A, Heijnen CJ, Albrecht PJ, Dougherty PM. Dorsal root ganglion infiltration by macrophages contributes to paclitaxel chemotherapy induced peripheral neuropathy. J Pain. 2016; doi: 10.1016/j.jpain.2016.02.011

Zhang T, Yao S, Wang P, Yin C, Xiao C, Qian M, Liu D, Zheng L, Meng W, Zhu H, Liu J, Xu H, Mo X. ApoA-II directs morphogenetic movements of zebrafish embryo by preventing chromosome fusion during nuclear division in yolk syncytial layer. J Biol Chem. 2011; 286:9514–9525. DOI: 10.1074/jbc.M110.134908 [PubMed: 21212265]

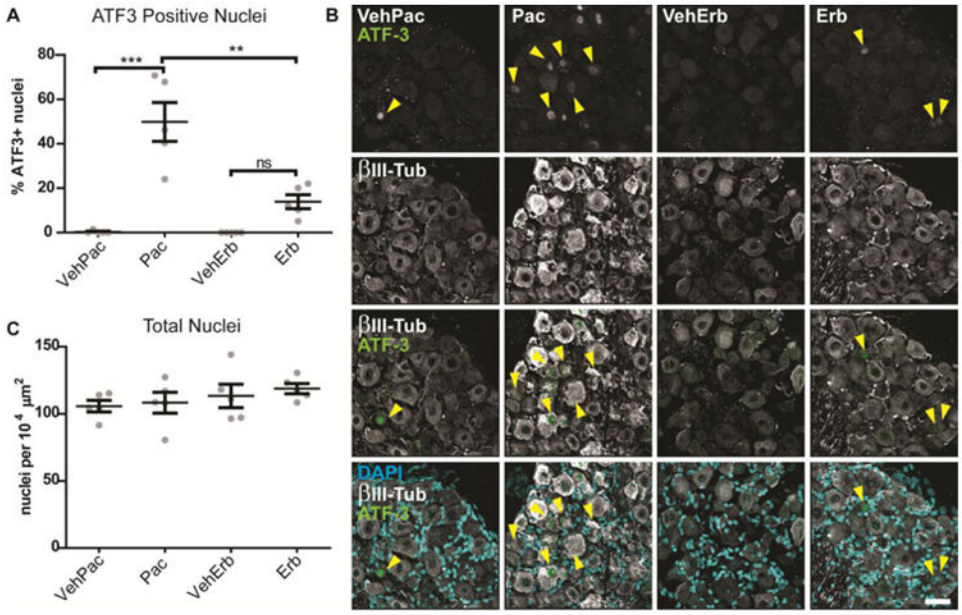

Figure 1. Paclitaxel increased the number of ATF3 positive DRG nuclei, while the total number of DRG nuclei remained unchanged by either drug

a Quantification of ATF3 positive nuclei per 10^4 μm^2 DRG tissue (n=5, **p < 0.01, ***p < 0.001). Error bars represent standard error of the mean (SEM). **b** Representative images, in merged images, ATF3 is represented in green, DAPI is represented in cyan, and βIII-tubulin is represented in white. Examples of ATF3 positive nuclei are indicated by yellow arrowheads. Scale bar 50 μm. **c** Quantification of total number of DAPI positive nuclei present per 10^4 μm^2 DRG tissue (n=5, p > 0.05), error bars represent SEM.

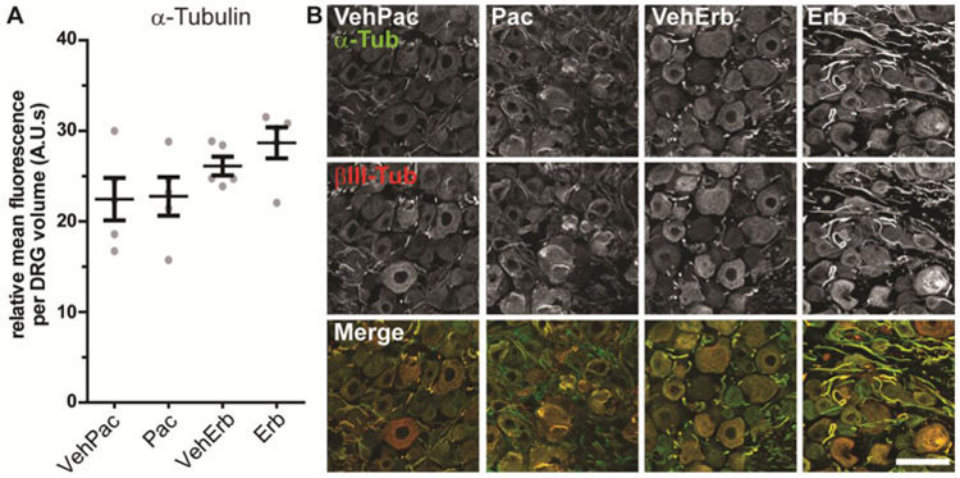

Figure 2. Neither paclitaxel nor eribulin altered levels of total tubulin in DRG neurons

a Quantification of the relative level of total tubulin as indicated by anti α-tubulin signal within neuronal cells. Error bars represent standard error of the mean. **b** Representative images. In merged images, α-tubulin signal is represented in green and βIII-tubulin is represented in red. No statistically significant changes were observed between any drug or vehicle treatments ($p > 0.05$). Scale bar 50 μm. N=5.

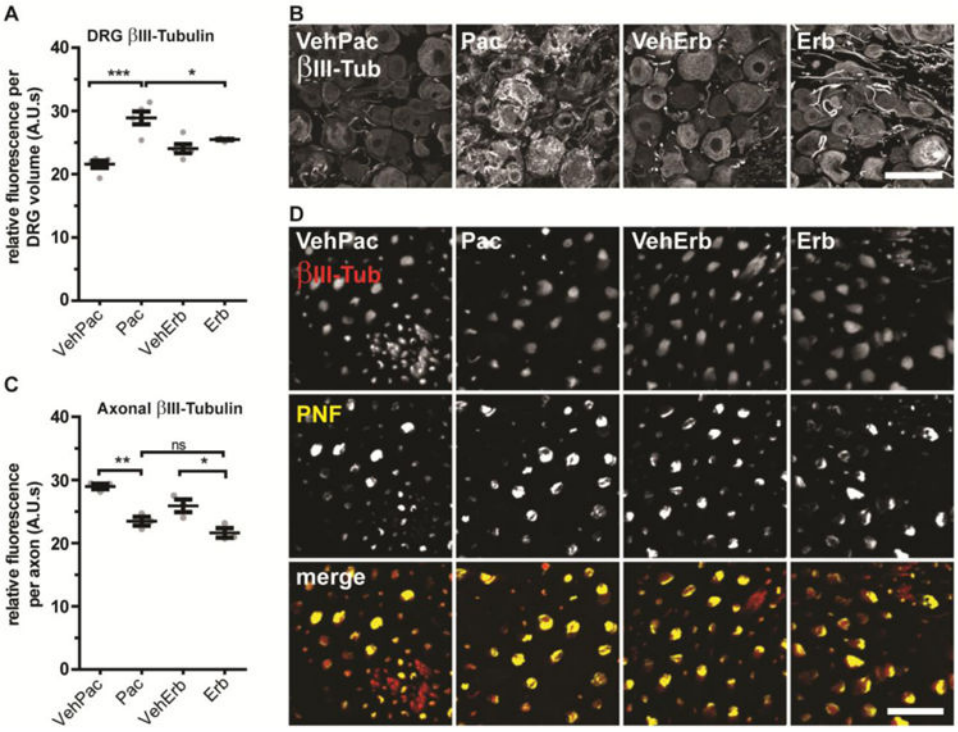

Figure 3. Paclitaxel increased βIII-tubulin in DRG, whereas both drugs reduced βIII in sciatic nerve axons

a Quantification of βIII-tubulin fluorescent signal in βIII-tubulin positive DRG neuronal volumes. Error bars represent standard error of the mean (SEM). (n=5, *p < 0.0167, ***p < 0.0003, Bonferroni corrected Student T-Test for multiple comparisons). **b** Representative images of DRG neurons from mice treated with paclitaxel, eribulin and their respective vehicles. Scale bar 50 μm. **c** Quantification of βIII-tubulin signal mean fluorescent signal of volumes positive for phosphoneurofilament (PNF) in axons of sciatic nerve tissue. Error bars represent SEM. (n=3, *p < 0.05, **p <0.001, ANOVA and post-hoc Tukey's test). **d** Representative images of sciatic nerve axons. In merged images βIII-Tubulin is red and phosphoneurofilament (PNF) is yellow. Scale bar 20 μm.

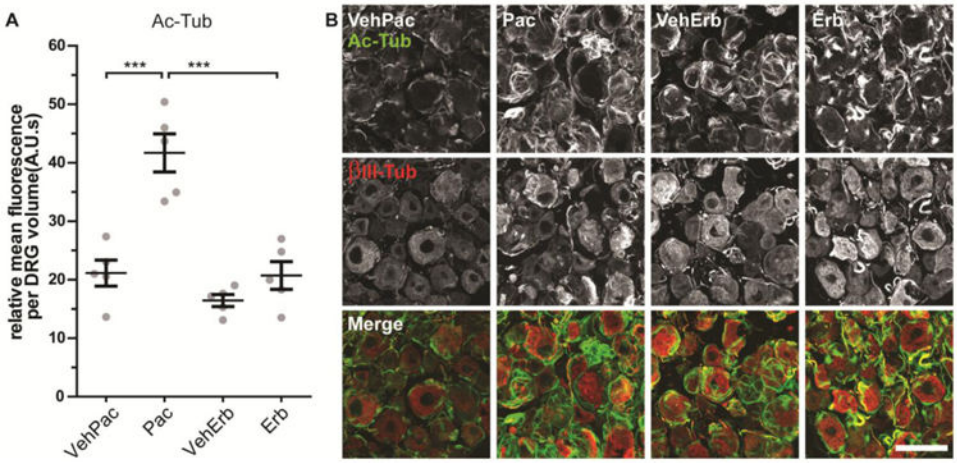

Figure 4. Paclitaxel but not eribulin increased levels of tubulin acetylation in DRG neurons

a Quantification of the relative mean levels of acetylated tubulin in the cell bodies of DRG neurons as defined by βIII-tubulin positivity. Error bars represent the standard error of the mean. (n=5, *** $p < 0.001$). **b** Representative images of tissue from all four treatment groups, In merged images, acetylated tubulin is green and βIII-tubulin is red. Scale bar 50 μm.

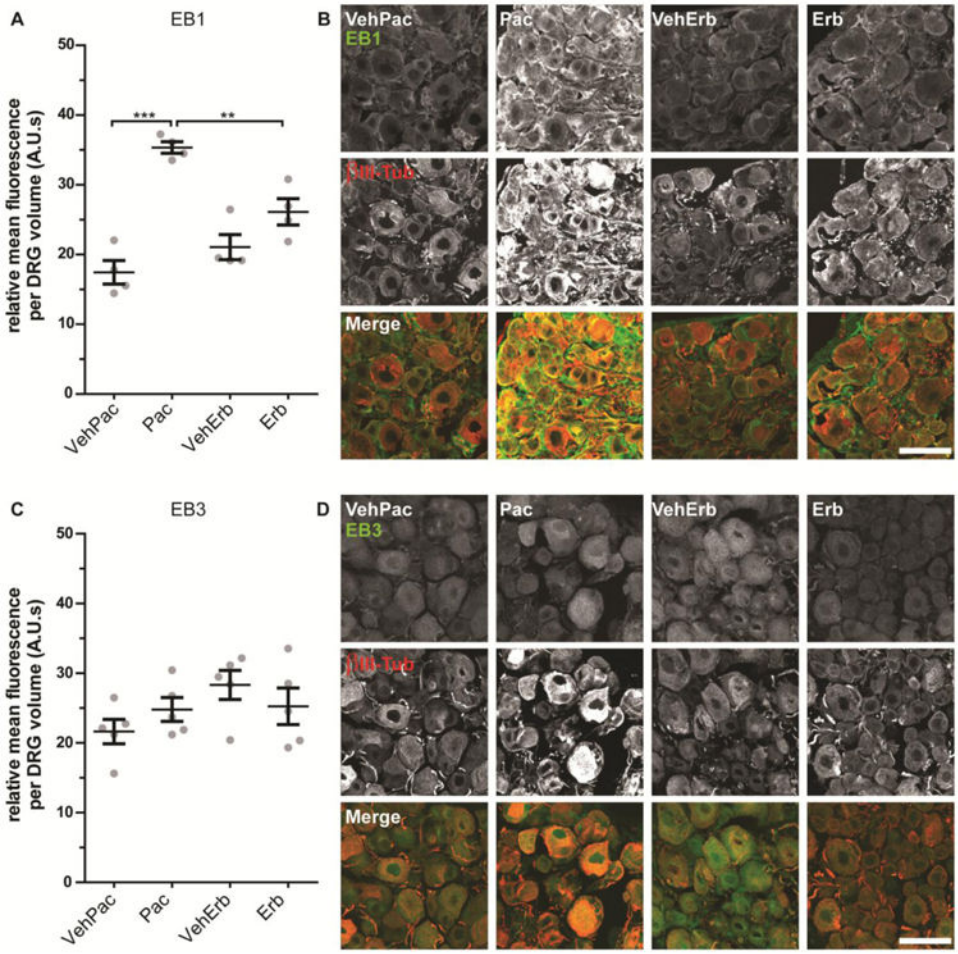

Figure 5. Paclitaxel increased the level of neuronal EB1 in DRG tissue, whereas neither paclitaxel nor eribulin altered levels of EB3

a Quantification of relative means of EB1 fluorescence in βIII-tubulin positive volumes across paclitaxel, eribulin and their respective vehicle conditions. Error bars represent the standard error of the mean (SEM). (n=4, **p < 0.01, *** p < 0.001). **b** Representative images of tissue from treated mice. In merged images, EB1 signal is represented in green and βIII-tubulin is represented in red. **c** Quantification of relative mean fluorescence levels of EB3 immunostaining. No statistical difference between means was found (n=5, p > 0.05). Error bars represent the SEM. **d** Representative images of tissue from treated mice. In merged images, EB3 signal is represented in green and βIII-tubulin is represented in red. Scale bars 50 μm.

Table 1

Fold change in protein levels

	Paclitaxel/Vehicle		Eribulin/Vehicle	
	DRG	**Sciatic**	**DRG**	**Sciatic**
α-Tub	1.01	1.9	1.09	2.6
Ac-Tub	1.9	4.6	1.2	11.7
EB1	2.02	1.1	1.2	2.2